

INFLUENCE OF PROJECTILE NOSE SHAPE ON BALLISTIC LIMIT AND DAMAGE TO GLASS/VINYL ESTER COMPOSITE PLATES

M. Sasikumar¹, V. Sundareswaran²

¹Research Scholar, Department of Mechanical Engineering, Anna University, Chennai -25. India.

E-mail: msasikumar@msn.com

²Professor, Engineering Design Division, Anna University, Chennai -25. India.

Received 1 June 2011; accepted 28 July 2011

ABSTRACT

In the recent past, the substantial structural strength, light weight and stiffness properties of polymer based composite materials find its application in aircraft and automotive structures at prodigious rate. Fibre glass Reinforced Plastic (FRP) composites are partially elastic and brittle. The present study evaluates the ballistic limit, energy absorbed and the damage area caused by different projectile nose shapes on the composite plates made of glass fibre and vinyl ester resin with the orientation of (0/90)_s. The number of plies in the plates is varied to 4, 6 and 8 and thus lead to different thicknesses. The projectile nose geometry is varied (hemispherical, conical, truncated conical, ogival and truncated ogival) to have realistic effect on the impact. The influence of projectile nose shape over ballistic limit is found experimentally and compared with the analytical predictions by H. M. Wen [5,6]. The ballistic limit, perforation mechanism, energy absorption at ballistic limit and the damage area at ballistic limit velocity has been studied. The influence of thickness of the composite plate over the ballistic limit have also been discussed. It is found that the truncated conical nose shaped projectile resulted in highest ballistic limit and largest damage area dominated by delamination. Experimental results showed that the analytical method [5,6] could satisfactorily predict the ballistic limit.

Keywords: composite plates, projectile shape, thickness of the plate, ballistic limit and the damage area.

1. INTRODUCTION

Fibre reinforced plastic composites are widely used in aerospace, marine and automotive structures due to their high specific strength, light weight and stiffness. Many researchers [1-4] have studied the low velocity impact of projectiles on composite plates made with glass fibre and epoxy. They have found the effect of projectile mass, orientation of fibres, laminate thickness and the boundary conditions. However, medium velocity impacts with various projectile nose shapes are of equal interest in the automobile field since the collision of automobiles with the obstacles is influenced by medium velocity impacts. The structures of interest in many applications are commonly composed of carbon/graphite, Kevlar and glass fibre reinforced polymer matrix composites. Among these the glass fibre is superior to the carbon fibre as they have low modulus, comparable strength and weaker interface between fibre and matrix.

The present study investigates the influence of projectile nose shape over ballistic limit, damage propagation, energy absorption and the damage area created in glass fibre/vinyl ester composite plates. Studies have addressed the effect and optimization

of projectile nose shape during the ballistic impact of fibre reinforced plastic plates [5-17].

Wen [5,6] has developed analytical equations for predicting the penetration and perforation of different nose shaped projectiles. He has developed models based on the assumptions that deformations during ballistic limit are localized and that the plates resist the impact by quasi-static resistive pressure and dynamic resistive pressure.

Ben- Dor et al [7] proposed a model to describe the penetration of FRP laminate by a rigid projectile. A numerical procedure was used to determine the shape of the impactor that penetrates at a given depth of penetration with the minimum and maximum impact velocity. The model suggested here generalizes the wen's model to the impactors having an arbitrary shape. It is found that, a flat nosed cylinder requires the maximum impact velocity.

Ben- Dor et al [8] derived a model for describing penetration of monolithic semi-infinite and finite FRP laminates struck transversely by a rigid projectile with an arbitrary 3-D shape. They have predicted the advantage of 3-D conical impactors over

conical impactors having the shape of the body of revolution.

Ben-Dor et al [9] proposed a model to describe the importance of depth of penetration over the nose shape of the projectile. They have found that the optimal nose geometry of the impactor varies and become close to a blunt cone with the increasing depth of penetration.

Lee and Sun [10] have performed an experimental and numerical study on carbon fibre reinforced plastic laminates impacted by flat ended projectiles. They have identified that the penetration process takes place in the following steps – pre-delamination, post delamination before plugging and post plugging. A computational model was developed to predict the ballistic characteristics of carbon fibre reinforced plastic plates.

Cantwell et al [11] found that, in thin specimens, the damage is initiated in the bottom layers, whereas with thick specimens, damage is initiated in the top layers. They have shown that the critical force increases with the indenter diameter and is more significant in thinner laminates.

Mitreviski et al [12] studied the effect of impactor shape on the impact response of composite laminates. All the composite laminates are tested with impact energies of 4J and 6J using hemispherical, ogival and conical impactors. It is found that the hemispherical impactor produced the highest peak force and lowest contact duration.

Mines et al [13] found that flat and hemispherical impactors produced bigger delamination areas compared to conical impactor in woven and z- stitched laminates of different thickness. It was also suggests that the damage caused by conical impactor is more localized.

Zhou et al [14] found that the change in indenter nose shape resulted in change in failure mode. It was found for most hemispherical indenters, the matrix crack was followed by the fracture of fibre. Ply shear out was found to be a major failure mechanism with the flat indenter.

Gellert et al [15] presented post perforation micro structural measurements for flat, conical, and fragment simulating projectiles of different dimensions impacting glass reinforced plastic laminates. It was shown that the energy absorption in thin glass rein-

forced plastic laminates is independent of the projectile shape.

Ulven et al [16] evaluated the perforation and damage evolution created by various projectile geometries in VARTM processed carbon/epoxy laminates. They have found that the panel thickness has a significant effect on the ballistic limit of panels impacted by different nose shaped projectiles. They have also observed failure mechanisms of plugging, separation of fibres, or a combination of both on the carbon/epoxy laminates.

Reyes Villanueva et al [17] studied about the high velocity impact response of a range of novel aluminium foam sandwich structures. The ballistic limit of the sandwich structures were predicted using a simple analytical model. They have also shown that these novel systems offer excellent energy absorbing characteristics under high velocity impact loading conditions.

2. SPECIMEN PREPARATION

The composite plates are manufactured from stitched type glass fibre and vinyl ester resin by hand lay up method. The glass fibre strands are stitched together by thin wire to form a unidirectional stitched mat of weight 750 g/m². The fibre mat is placed in the required orientation and the resin is impregnated into fibre by nip-roller type impregnators. The stacking sequence of the fibre mat is given in the Table 1. Then the resin is forced into the fabrics by means of rotating rollers on a bath of resin. Laminates are left to cure under standard atmospheric conditions. Composite plates of three different thicknesses with 4, 6 and 8 plies were fabricated. The post curing is carried out at 80 °C for 4 hours. It is then cooled to room temperature at atmospheric pressure. Once cured the panels were cut into specimens of 210x210 mm in dimension.

Table 1: Details of specimens

Stacking sequence	No. of layers	Average Thickness(mm)
(0/90) _{2S}	4	3.64
(0/90/0) _{2S}	6	5.35
(0/90/0/90) _{2S}	8	7.1

3. EXPERIMENTAL METHOD

3.1. Impact setup

Medium velocity impact tests were conducted using a new pneumatic test rig equipped with digital counters is shown in Fig. 1. The set up is designed and fabricated to push the projectile with high and variable velocities using compressed air. Projec-

tiles placed at the end of the tube were propelled by compressed gas when an electromagnetic valve was opened that exposed the projectile's rear end to the reservoir pressure. Velocity attained depends on the mass of the projectile, pressure applied to the projectile and the friction present in between the projectile and the guide pipe while moving inside the pipe. Here, by keeping the friction factor of the mass of the projectile constant, the pressure is varied to achieve different velocities. Two digital counters are used to measure the initial velocity and the residual velocity of the projectile.

The specimen, which was prepared earlier, was mounted in a fixture and clamped on all four sides to provide an impact area of 180x180 mm. A simple technique was developed in the present investigation for the measurement of initial velocity. Two thin wires are kept in the path of the projectile inside the guiding pipe. The two ends of the wires were connected to power source, which in turn was connected to a digital counter to form a closed circuit. When the projectile cuts the first wire, it triggered the digital counter and the counter was stopped when the projectile cuts the second wire. From the counter reading and the distance between the wires, the initial velocity of the projectile was calculated. The same technique with minor modification was used to find the final velocity of the projectile. Since the path of the projectile was unpredictable after penetration, the wires were wound over square frames of size 300x300 mm and kept at a known distance below the specimen to measure the projectile velocity after the impact. The initial and final kinetic energy of the projectile were calculated. Using the



Fig. 1: Experimental set up

initial and final kinetic energy, energy absorption of the plate was computed. The ballistic limit was determined experimentally by conducting the impact test at different initial velocities. The ballistic limit velocity v_b is considered as the velocity at which the projectile has emerged from the back face but still remains embedded in the composite plate.

3.2. Projectile

The projectiles are made of stainless steel and polished to have smooth surface area. The nose geometry of the projectile is varied to hemispherical, conical, truncated conical, ogival and truncated ogival without changing the mass of the projectile as shown in the Fig. 2. The length of the projectiles is obtained in between 70 to 74 mm to have constant mass for all the projectiles. The parameters of the projectile are listed in the Table 2.

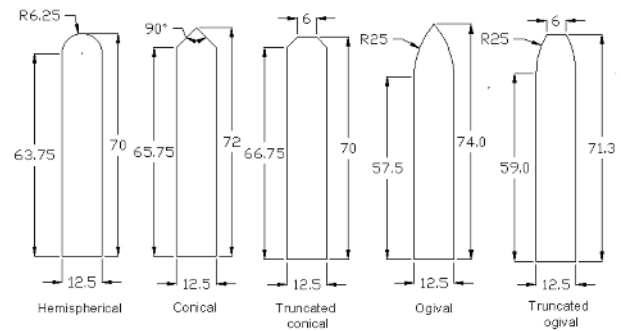


Fig. 2: Projectile shape and dimensions

Table 2: Details of the projectile

Stacking sequence	No. of layers	Average Thickness(mm)
(0/90)2s	4	3.64
(0/90/0)2s	6	5.35
(0/90/0/90)2s	8	7.1

3.3. Quasi-static test

Quasi-static tests were performed on the samples of the composite plates that were cut from the same panels. All the plates tested were orthotropic in nature having a symmetrical lay-up about its mid plane. Tensile strength, shear strength and flexural strength were determined using Universal Testing Machine. Izod impact test was performed on the sample plate using Izod impact testing machine. Short beam test was performed to find out the shear strength of the plate. All the tests were carried out according to ASTM standards and listed in Table 3.

4. RESULTS AND DISCUSSION

4.1 Damage area

The damaged specimens are inspected visually to assess the damage occurred such as matrix cracking, fibre breakage and delamination. The extent of

Table 3: Properties of the composite plate

Material properties	Measure
Young's modulus (E_1)	16.03 GPa
Young's modulus (E_2)	4.18 GPa
Major Poisson ratio (ν_{12})	0.27
Minor Poisson ratio (ν_{21})	0.054
Tensile strength (σ_t)	136.68 MPa
Compressive strength (σ_c)	306.83 MPa
Inter laminar shear strength (G_{12})	7.1 MPa
Density (ρ)	1209.09 kg/m ³
Interlaminar fracture toughness (G_{II})	3.82 kJ/m ²
Energy density (E_d)	15 MJ/m ²
Frictional force (F_f)	250 N

delamination is used to evaluate the total damage area created by different nose shaped projectiles at their ballistic limit velocities. The extent of the damage area is measured by exposing the impacted composite plate against a bright light source. All types of damages scatter the light and make the damaged area opaque. The front face of the composite plates is shown in the Figs. 3, 4 and 5. For the conical, ogival and hemispherical projectile, the fibre strands in the upper layers of the plate under the projectile impact face undergone failure and provided the way for the projectile to penetrate into the composite plate (Figs. 3, 4 and 5). But the bottom layer of the plate has undergone stretching, separation of fibre strands followed by elastic-plastic hole enlargement. Figs. 6, 7 and 8 illustrate the back face damage for the 7.1 mm, 5.35 mm and 3.64 mm plates respectively. For truncated conical and truncated ogival, due to large impact face, fibre in all the layers except bottom layer have undergone plugging. However, the extent of the delamination is more on the bottom layer than the top layer of the plate for all the projectiles. The damaged area is mapped on to a graph sheet (Fig. 9) and is measured with respect to the back face of the composite plate. Table 4 summarizes the damage observations at ballistic limit velocity for each specimen.

In the 7.1mm thick plates, the average damage area in the plates was the largest due to the impact of truncated conical projectile(13%greater) followed by truncated ogival(11% greater), hemispherical(37% greater), conical(17% greater) and ogival projectiles(Fig. 10). Due to the small variation in the ballistic limit and damage area, penetration of composite plates by different nose shaped projectiles is significantly dependent on panel thickness. The influence of projectile nose geometry is higher for the thicker specimens. The thicker plates have

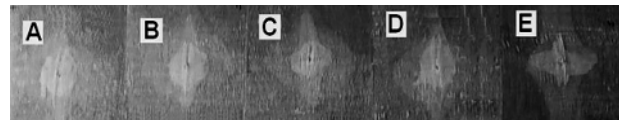


Fig. 3: Front face damage of (A) truncated conical, (B) truncated ogival, (C) hemispherical, (D) conical, (E) ogival for 7.1 mm plates.

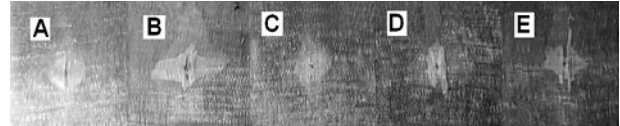


Fig. 4: Front face damage of (A) truncated conical, (B) truncated ogival, (C) hemispherical, (D) conical, (E) ogival for 5.35 mm plates.

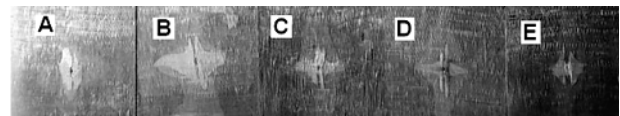


Fig. 5: Front face damage of (A) truncated conical, (B) truncated ogival, (C) hemispherical, (D) conical, (E) ogival for 3.64 mm plates.

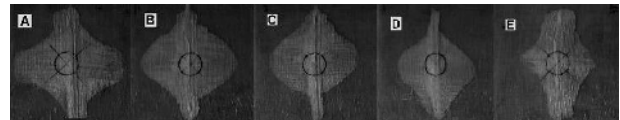


Fig. 6: Back face damage of (A) truncated conical, (B) truncated ogival, (C) hemispherical, (D) conical, (E) ogival for plates of 7.1 mm plates.

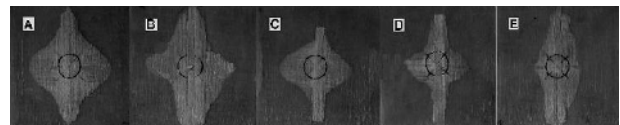


Fig. 7: Back face damage of (A) truncated conical, (B) truncated ogival, (C) hemispherical, (D) conical, (E) ogival for plates of 5.35 mm plates.

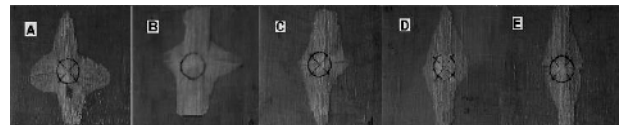


Fig. 8: Back face damage of (A) truncated conical, (B) truncated ogival, (C) hemispherical, (D) conical, (E) ogival for plates of 3.64 mm plates.

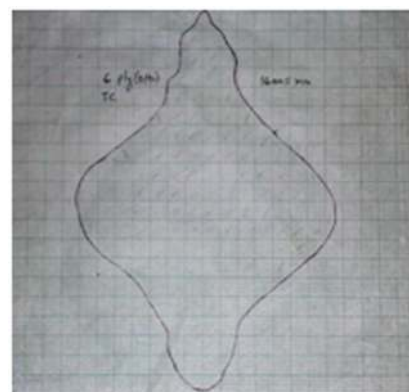


Fig. 9: Damage area of 5.35 mm plate plotted on graph sheet for truncated conical

Table 4: Damage area at ballistic limit

Plate thickness (mm)	Nose shape of the projectile	Average Damage area at ballistic limit (mm ²)
3.64	Truncated Conical	11780
3.64	Truncated Ogival	10402
3.64	Hemispherical	9800
3.64	Conical	8712
3.64	Ogival	8478
5.35	Truncated Conical	16005
5.35	Truncated Ogival	13964
5.35	Hemispherical	12382
5.35	Conical	9460
5.35	Ogival	8653
7.1	Truncated Conical	23992
7.1	Truncated Ogival	21168
7.1	Hemispherical	18678
7.1	Conical	15449
7.1	Ogival	10800

more stiffness and have less deflection during impact. Therefore, major portion of the impact energy is absorbed by the damage mechanisms.

Similarly, in the 5.35mm thickness, the average damage area in the plates was the largest due to the impact of truncated conical(14%greater) followed by truncated ogival(13% greater), hemispherical(30% greater), conical(9% greater) and ogival projectiles (Fig. 10).

In the 3.64 mm thickness, the range of average damage area is small (~10%) as the thin composite plates flex readily during the ballistic event and absorbs majority of the impact energy regardless of the shape of the projectile (Fig. 10). The influence of projectile nose geometry is found to significantly affect the ballistic resistance of the panels.

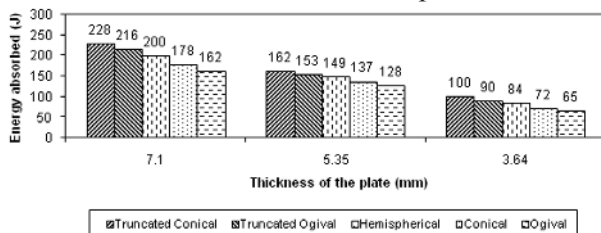


Fig. 10: Damage area (%) at ballistic limit velocity for each specimen

4.2 Energy Absorption

The incident energy is absorbed completely by the composite plate until reaching the ballistic limit and beyond the ballistic limit the energy absorbed increases for a certain value of incident energy. As the incident velocity increases, further the energy absorption decreases for each specimen. At velocities slightly above the ballistic limit, there is enough time for the laminates to undergo deflection and absorbs more energy. But at higher velocities, laminates undergo deflection to a smaller extent and thus

absorbs less energy.

In the 3.64 mm thick specimens, at ballistic limit, the largest amount of energy absorbed in the plate occurred from the impact of truncated conical projectile (11% greater) followed by the truncated ogival (7% greater), hemispherical (17% greater), conical (10% greater) and ogival projectile (Fig. 11). The ogival and conical projectiles penetrate with lower velocity because they initially create a small shear zone followed by elastic and plastic hole enlargement. Failure in the plates impacted with the ogival, conical and hemispherical projectiles results in elastic and plastic hole enlargement where the fibres are more likely to spread and stretch during penetration. So, the plates impacted by ogival, conical and hemispherical projectiles absorb less energy. During impact, truncated conical projectile also creates a shear zone which results in fibre pull out and plugging. But the energy absorbed in it is much greater due to the large impact face. However, due to large surface area on the hemispherical projectile, part of the failure is also a result of shear loading of the laminate. The energy absorbed by each plate increases with the increase in the damage area.

In the 5.35 mm thick specimens, energy absorbed is narrow, yet the amount of energy absorbed is higher than the 3.64 mm thick specimens for all the different nose shaped projectiles. The largest amount of energy absorbed in the plate occurred from the impact of truncated conical projectile (5% greater) followed by the truncated ogival (3% greater), hemispherical (9% greater), conical (6% greater) and ogival projectile (Fig. 11).

The 7.1mm thick specimens absorb more than those of 5.35 and 3.64mm thick specimens for all the different nose shaped projectiles. The largest amount of energy absorbed in the plate occurred from the impact of truncated conical projectile (6% greater) followed by the truncated ogival (8% greater), hemispherical (12% greater), conical (9% greater) and ogival projectile (Fig. 11).

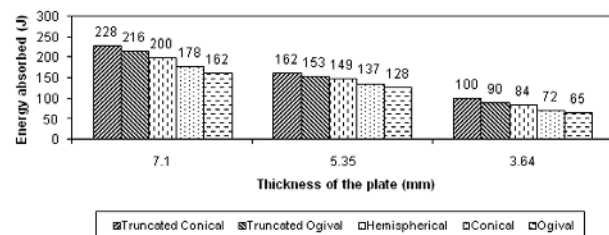


Fig. 11: Energy absorbed at ballistic limit velocity for each specimen

4.3 Ballistic limit velocity

Wen's analytical equations [5,6] were used to predict the ballistic limit of the composite plates impacted by different nose shaped projectiles. The average stress provided by the FRP against the projectiles is divided into two parts. One part is the cohesive quasi-static resistive stress (σ_s) applied normally to the projectile surface due to elastic-plastic deformation of the laminate materials and the other is dynamic resistive stress (σ_d) due to velocity effects. The mean pressure applied (σ) is expressed as

$$\sigma = \sigma_s + \sigma_d \tag{1}$$

It is also assumed that cohesive quasi-static stress is equal to the quasi-static linear elastic limit σ_e in through thickness compression of the FRP laminates. i.e. $\sigma_s = \sigma_e$ and the dynamic resistive pressure is taken as $\beta v_i \sigma_e \sqrt{\ell_l / \sigma_e}$. The equation (1) becomes

$$\sigma = \sigma_e \left[1 + \beta v_i \sqrt{\frac{\ell_l}{\sigma_e}} \right] \tag{2}$$

Where β is a constant, determined empirically [5]. For conical, $\beta = 2 \sin(\theta/2)$ and for ogival and hemispherical, $\beta = 3/(4\psi)$ and $\psi = S / 2r_p$

From energy consideration, we get

$$E_i = \int_0^{D_p} F_r dD_p \tag{3}$$

Where E_i is the initial kinetic energy of the projectile. Substituting for F_r in the equation (3) and applying β for different nose geometries, we get the ballistic limit of the plate for different nose shaped projectiles as follows:

Hemispherical ($S = r_p$ and hence $\beta = 3/2$):

$$v_b = \frac{3\pi d_p^2 t \sqrt{\ell_l \sigma_e}}{8m} \left[1 + \sqrt{1 + \frac{32m}{9\pi \ell_l d_p^2 t}} \right] \tag{4}$$

Conical:

$$v_b = \frac{\pi \sin(\theta/2) d_p^2 t \sqrt{\ell_l \sigma_e}}{2m} \left[1 + \sqrt{1 + \frac{8m}{\pi \beta^2 \ell_l d_p^2 t}} \right] \tag{5}$$

Ogival ($S = 4r_p$ and hence $\beta = 3/8$):

$$v_b = \frac{3\pi d_p^2 t \sqrt{\ell_l \sigma_e}}{32m} \left[1 + \sqrt{1 + \frac{512m}{9\pi \ell_l d_p^2 t}} \right] \tag{6}$$

The truncated conical projectile is having both flat surface and conical surface. So, the resistive pressure of the composite plate for the truncated conical projectile is expressed as $\sigma_f a_t + \sigma_c (a - a_t)$, summation of resistive pressures offered to the flat and conical surface of the projectile. Hence, we get ballistic limit for truncated conical projectile as

$$v_b = \sqrt{\frac{2\pi r_p^2 t \sigma_c}{m} \left[1 + \left(\frac{\sigma_f}{\sigma_c} - 1 \right) \left(\frac{r_t}{r_p} \right)^2 \right]} \tag{7}$$

Similarly, for truncated ogival

$$v_b = \sqrt{\frac{2\pi r_p^2 t \sigma_o}{m} \left[1 + \left(\frac{\sigma_f}{\sigma_o} - 1 \right) \left(\frac{r_t}{r_p} \right)^2 \right]} \tag{8}$$

The parameters used in predicting the ballistic limit are given by

- σ_f - Mean resistive pressure of the plate for flat nose shaped projectile
- σ_c - Mean resistive pressure of the plate for conical nose shaped projectile
- σ_o - Mean resistive pressure of the plate for ogival nose shaped projectile
- v_i - Initial velocity of the projectile.
- v_b - Ballistic limit velocity
- d_p - Diameter of the projectile
- r_p - Radius of the shank portion of the projectile
- r_t - Radius of the truncated portion of the projectile
- m - Mass of the projectile
- ℓ_l - Density of the composite plate.
- D_p - Depth of penetration.
- F_r - Resistive pressure of the plate
- t - Thickness of the composite plate
- ψ - Caliber-radius head
- θ - Cone angle of the conical projectile
- a_t - Cross sectional area of the truncated part
- S - Radius of the ogive and hemisphere

The ballistic limit of the composite plates of 3.64, 5.35 and 7.1mm thickness are predicted using Wen's analytical models and compared with the experimental results. The ballistic limit of the plates of different thickness obtained from analytical and experimental methods follow the same trend. However the analytical method overestimates the ballistic limit obtained from experimental method. For the 3.64 mm thick plates, the ballistic limit found by analytical method is deviated from the experimental values in the range of 8% to 18%, (Fig. 12) for 5.35 mm thick plates, the deviation is in the range of 3% to 6%, (Fig. 13) and for 7.1 mm thick plates, the de-

variation is in the range of 2% to 10%(Fig. 14).

The difference in ballistic limit found by the analytical model and the experimental method is due to manufacturing method (hand layup method) of the composite plate, boundary conditions (clamping force) and the failure mechanisms. Also, the shearing caused by the crimping and undulations of the fibre mat decreases the ballistic limit.

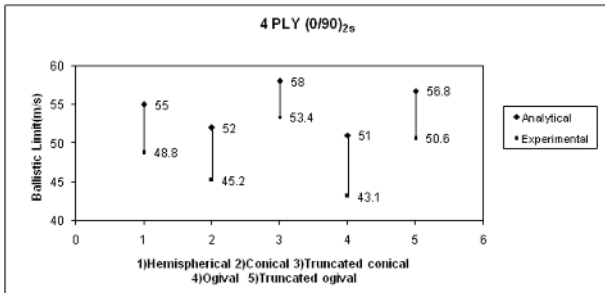


Fig. 12: Predicted and experimental ballistic limit velocity of the 3.64 mm plates

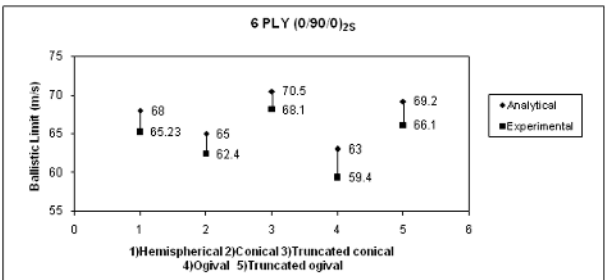


Fig. 13: Predicted and experimental ballistic limit velocity of the 5.35 mm plates

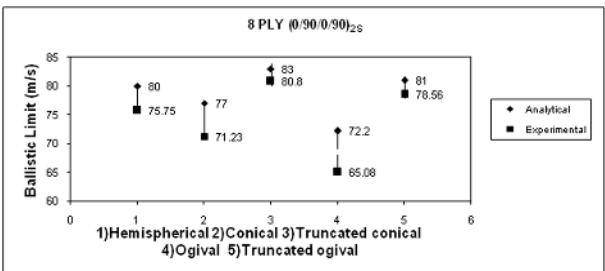


Fig. 14: Predicted and experimental ballistic limit velocity of the 7.1 mm plates

5. SUMMARY

The influence of different nose shaped projectiles on the glass/ vinyl ester composite plates under medium velocity impact resulted in a range of energy absorptions at ballistic limit. Truncated conical projectile resulted in highest energy absorption at ballistic limit followed by truncated ogival, hemispherical, conical and ogival projectile. A combination of failure mechanisms such as matrix cracking, fibre breakage, separation of fibres, delamination and plugging were observed under the impact of dif-

ferent nose shaped projectiles. The thickness of the composite plate has a significant effect on the ballistic limit velocity, impacted by different nose shaped projectiles. The thicker plates have more stiffness and have less deflection during impact and thus major portion of the impact energy is absorbed by the damage mechanisms. The thin composite plates flex readily during the ballistic event which absorbs majority of the impact energy regardless of the shape of the projectile. The trend of ballistic limit for the glass/vinyl ester composite plates impacted by different nose shaped projectiles was predicted using Wen's analytical model and it was compared with the experimental method. Deviations were higher for thinner composite plates than the thicker ones.

References:

1. Lam K.Y and Sathiyamoorthy T.S Response of composite beam under low velocity impact of multiple masses. *Composite structures* **44** (1999), 205-220
2. Belingardi G. Vadori R. low velocity impact tests of laminate glass-fibre epoxy matrix composite material plates. *Int. J Impact Engg.* **27** (2002), 213-229
3. Zuleyha Aslan, Ramazan Karakuzu, Buket Okutan, The response of laminated composite plate under low velocity impact loading. *Composite structures* **59** (2003), 119-127
4. Sutherland. L.S, Guedes Soares.C, Impact on low fibre volume, glass/polyester rectangular plates, *Composite structures* **68** (2005), 13-23
5. H.M. Wen. Predicting the penetration and perforation of thick FRP laminates struck normally by projectile with different nose. *Composite structures.* **49** (2000), 321-329.
6. H.M. Wen. Penetration and perforation of thick FRP laminates, *Composite structures* **61/8** (2001),1163-1172
7. Ben-Dor. G, Dubinsky. A, Elperin. T, Optimal nose geometry of the impactor against FRP laminates, *Composite structures* **55** (2002), 73-80
8. Ben-Dor. G, Dubinsky. A, Elperin. T, A model for predicting penetration and perforation of FRP laminates by 3-D impactors, *Composite structures* **56** (2002), 243-248
9. Ben-Dor. G, Dubinsky. A, Elperin. T, Optimization of the nose shape of an impactor against a semi infinite FRP laminate, *Composite Science and technology* **62** (2002), 663-667.
10. Lee S. W. R, Sun C. T, dynamic penetration of graphite/epoxy laminates impacted by a blunt ended projectile. *Composite science and technology* **49** (1993), 360-380.
11. Cantwell W. J, Morton J, Impact perforation of CFRP, *Composite Science and technology* **38** (1990), 119-141.
12. Mitrevski. T, Marshall. I. H, Thomson. R, The in-

- fluence of impactor shape on the damage to composite laminates. *Composite structures* **76** (2006), 116-122.
13. **Mines R. A. W, Roach A. M, Jones N**, High velocity perforation behavior of polymer composite laminates. *Int J Impact Engineering* **22** (1999), 561-588.
 14. **Zhou G, Lloyd J. C, McGuirk J. J**, Experimental evaluation of geometric factors affecting damage mechanisms in carbon/epoxy plates. *Comp. Part A: Applied science Manufacturing* **32** (2001), 71-84.
 15. **Gellert E. P, Cimpoeru S. J, Woodward R. L**. A study of the effect of target thickness on the ballistic perforation of glass fibre- reinforced plastic composites. *Int. J Impact Engineering* **24** (2000), 445-456.
 16. **Ulven. C, Vaidya. U.K and Hosur. M**, effect of projectile shape during ballistic perforation of VAR-TM carbon/epoxy composite panels. *Composite Structures* **61** (2003), 143-150
 17. **Reyes Villanueva. G and Cantwell. W. J**. The high velocity impact response of composite and FML-reinforced sandwich structures. *Composite science and technology* **64** (2004), 35-54.